

# THE IFMIF HIGH ENERGY BEAM TRANSPORT LINE

Romuald Duperrier, Jacques Payet, Didier Uriot (CEA/DSM/DAPNIA, Gif-sur-Yvette)

## Abstract

The International Fusion Materials Irradiation Facility (IFMIF) project requests two linacs designed to accelerate 125 mA deuteron beams up to 40 MeV. The linac operates in CW mode and uses one RFQ and 10 DTL tanks [1]. After extraction and transport, the two deuteron beams with strong space charge forces have to be bunched, accelerated and transported to the target for the production of high neutron flux. This paper presents the High Energy Beam Transport (HEBT) line which provides a flat rectangular beam profile on the liquid lithium target. Transverse uniform beam density is obtained using non-linear multipole lenses (octupoles and duodecapoles). Optical design and beam dynamics with and without errors has been studied.

## INTRODUCTION

The two HEBT lines have to transport the beams to the Lithium liquid target, or to the dump, with the required footprint sizes and characteristics [2]. The footprint of each beam must be rectangular, 20 cm horizontal  $\times$  5 cm vertical at the flat top. The beam flux has to be approximately uniform ( $\pm 5\%$ ) across the flat top of the beam profile. Beyond  $\pm 11$  cm in horizontal, the beam density must be lower than  $0.5 \mu\text{A}/\text{cm}^2$ .

Each beam intercepts the target with an angle of  $9^\circ$ . This value results from a compromise between maximizing the flux in the test cell and minimizing the line activation due to back streaming neutrons [2]. The deviation is obtained with one achromat, composed of two  $4.5^\circ$  bends located near the accelerating system output.

The horizontal separation between the target centre and the linac reference line, needed for shielding consideration [3], is 5.3 m and the total line length is 43.12 m.

Optically, the HEBT line is divided in three functional sections [9]: a) the first section, which includes the achromat, matches the linac output beam through the achromat and for the entry in the second section; b) in the second section, the optical conditions are designed in order to allow for insertion of the octupole and duodecapole lenses at 4 positions; c) the last section, including the beam expansion drift, allows the matching of the needed beam sizes at the target.

This architecture allows an easy tuning of the line. All the first order simulations are performed with the code BETA [4]. In Figure 1 are shown the full HEBT line optical functions for a  $10 \text{ cm} \times 5 \text{ cm}$  footprint beam size at the target.

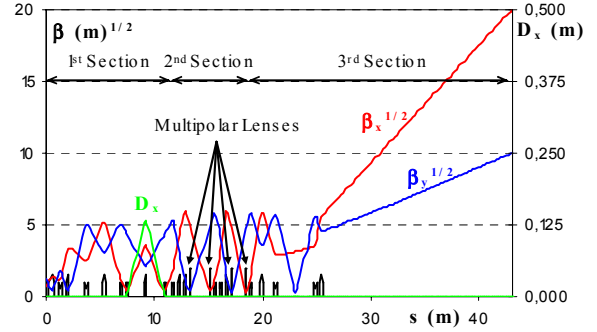


Figure 1: HEBT line optical functions.

## OCTUPOLE TUNING

The tuning of the octupoles [5] assumes the following hypothesis: a) the transverse motions are supposed to be uncoupled (the space charge coupling is assumed negligible); b) the non-linear lenses dedicated to the horizontal distribution flatness (respectively the vertical distribution) are supposed to be located at a waist of the vertical motion (respectively the horizontal). This allows acting on one plane with minimized effects on the other plane; c) at the horizontal non-linear lenses (respectively the vertical), the beam ellipses in the horizontal phase space ( $x, x'$ ) (respectively the vertical ( $z, z'$ )) is supposed to be thin enough ( $\beta_y \gamma_y \gg 1$ ,  $y=x, z$ ); d) the beam distribution is assumed to be gaussian.

Then, in the octupole case, the extent of the region of uniform density at the target is given by:

$$y_M = \pm \frac{8}{9} \sqrt{\epsilon_0 \gamma_0} \left( \frac{-\beta_0}{\alpha_0} T_{11} + T_{12} \right)$$

The octupole normalized strength  $OL$ , is given by:

$$OL = \frac{3}{16} \left( \frac{-\beta_0}{\alpha_0} T_{11} + T_{12} \right) / \left( \epsilon_0 \gamma_0 T_{12} \left( \frac{\beta_0}{\alpha_0} \right)^3 \right)$$

where  $\beta_0, \alpha_0, \gamma_0 = (1 + \alpha_0^2)/\beta_0$  are the optical functions at the lenses,  $\epsilon_0$  is the beam rms emittance,  $L$  is the octupole length and  $T_{11}, T_{12}$ , are the terms of the 1<sup>st</sup> order transfer matrix between the octupolar lenses and the target.

## PARTICLE IN CELL SIMULATION

### Calculation framework

A  $10^6$  macro particle 4D water-bag distribution is used at the input of the RFQ with a transverse rms normalised emittances of  $0.25 \pi \cdot \text{mm} \cdot \text{mrad}$ . The beam current is

130 mA. Multi-particle simulations are done from the RFQ output in the full DTL. And finally, the output DTL beam distribution is injected in the HEBT line.

Transport through the RFQs is done with TOUTATIS [6]. Transport through the rest of the linac and the HEBT is done with TraceWin / PARTRAN [7] (with PICNIC [8] 3D space-charge routine taking into account the bunch overlap effect).

The behaviour of the beam envelope in the HEBT is plotted below in Figure 2. Due to the halo beam size, induced by non-linear effect, we estimate that a beam pipe radius of  $15\sigma$  is necessary to fulfil the beam losses requirements.

Two octupoles and two duodecapoles are used to reach the footprint requirement. The duodecapole role is to improve the beam flatness by folding back the peaks created by the octupole [5].

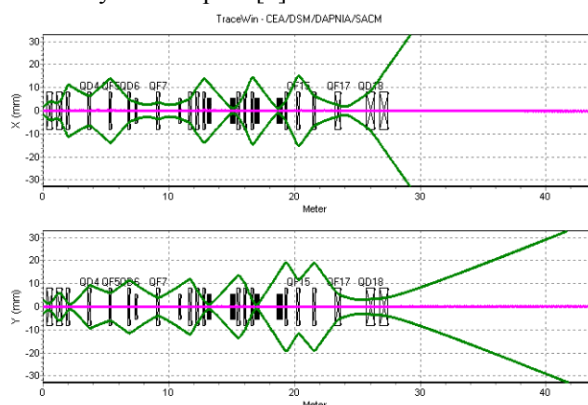


Figure 2: Transverse beam envelopes.

### Output distribution

The output profile is shown by Figure 3. These results indicate that the deviations from uniformity in the flat-top region are in the range of  $\pm 7\%$ , rather than the required  $\pm 5\%$  in vertical plane, while the horizontal beam distribution is better than required. The peaks along the horizontal edge rise are much better than the desired 15%. But the  $0.5 \mu\text{A}/\text{cm}^2$  beam density limit beyond  $\pm 11 \text{ cm}$  is clearly out of reach, especially in a space-charge regime.

### Beam losses

The simulation using the beam distribution from the DTL shows losses mainly located in the non-linear lenses, where the pipe radius is the smallest. About  $6 \mu\text{A}$  (240 W) are lost.

To avoid losses all along the HEBT and to minimize activation, a dedicated scraper can be designed to withstand more easily the losses and allow easier multipole element shielding. The simulation shows no loss if it is located after the achromat line. The removed beam portion corresponds to 0.02% (1 to 2 kW). The graphs in the Figure 4 represent the different beam size radii and the aperture along the HEBT, the black line includes all the macroparticles and the last black line represents the aperture. The scraper avoids the losses in the multipole lenses.

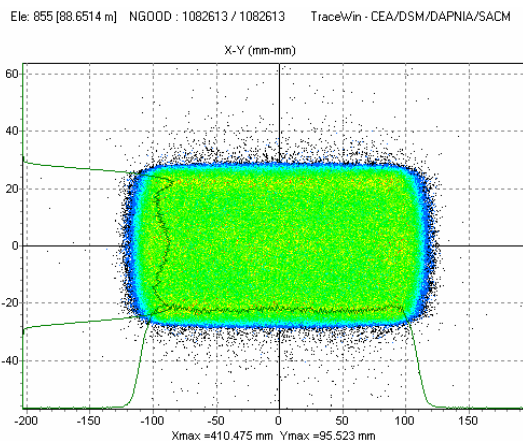


Figure 3: Output HEBT beam distribution at the target.

Taking into account this point and the beam size, it appears that losses will mainly occur from the last doublet to the target. By inserting a wall before this doublet, we avoid activation of the line induced by these losses and back-scattered neutrons from the target.

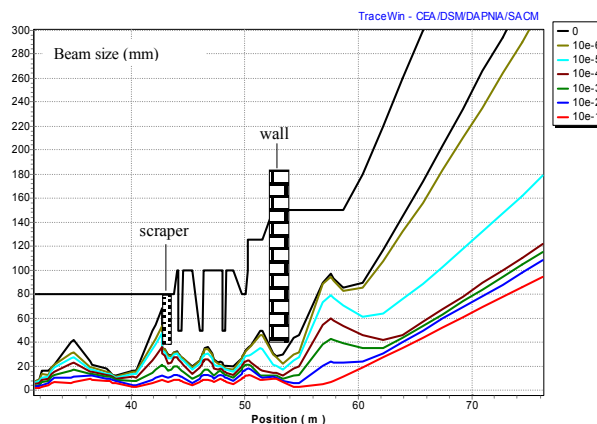


Figure 4: Beam size radii along the HEBT, without element errors ( $10^{-1}$  corresponds to 90% of the beam,  $10^{-2} \rightarrow 99\%$ ,  $10^{-3} \rightarrow 99.9\%$ , and the black one: 100%).

## ERRORS STUDIES

Two families of errors are taken into account [9]: a) static errors, the effect of these errors can be detected and cured with appropriate diagnostics and correctors; b) dynamic errors, the effect of these errors is assumed to be uncorrected.

There is no error on the dipole elements in the present study. At the present time, we did not include in our simulation specific correction for the gradient errors which cause mainly mismatching. Thus, we consider that the error study results below show a worse beam behaviour than the nominal operating mode.

### Correction scheme

A correction set is constituted of two steerers which are associated with two Beam Position Monitors (BPM). In

the HEBT, 6 correction-sets are necessary to control the beam central trajectory. The correction scheme is efficient in the DTL (residual orbit radius is lower than 1 mm) and in the first part of the HEBT line. Conversely, the correction of the last 17 m drift is more problematic due to the large optical functions.

The rms value of the residual orbit along the DTL and HEBT is plotted on Figure 5. It is the result of a set of statistics over 100 linacs. We notice that the rms jitter centroid position at the target is about 6 mm. It is due to the dynamic errors (vibrations: 5  $\mu\text{m}$  for DTL, 2  $\mu\text{m}$  for HEBT). In order to reduce the jitter, vibration tolerances have to be significantly reduced, although already challenging.

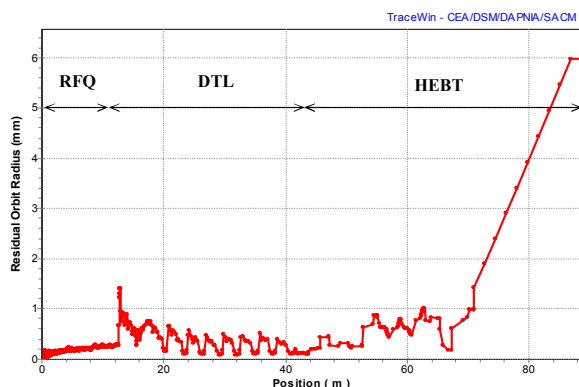


Figure 5: Residual orbit RMS value along the linac and the HEBT.

### The HEBT line

We study the HEBT line alone. The transport of a  $10^5$  macroparticle beam has been simulated in a set of 110 different HEBT lines with all combined errors on each element. Figure 6 show the statistical distribution of the particles along the HEBT, the black line includes all macroparticles and the last black line represents the aperture. We observe that 1.2 kW are dissipated in the scraper. For a pipe radius limited to 200 mm in the last drift, 1 particle over  $10^6$  will be lost.

The same studies were performed including the linac errors and show similar results [9].

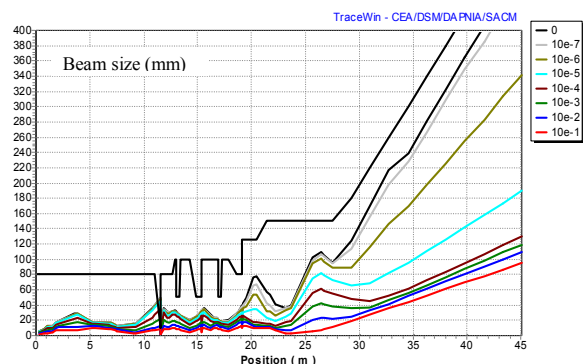


Figure 6: Beam size radii along the HEBT, with element errors ( $10^{-1}$  corresponds to 90% of the beam,  $10^{-2} \rightarrow 99\%$ ,  $10^{-3} \rightarrow 99.9\%$ , and the black one: 100%).

## CONCLUSIONS

We demonstrated the existence of a design for the IFMIF HEBT line. All the beam characteristics requirements at the target can be reached using multipole lenses, excepted for the horizontal beam density limit ( $0.5 \mu\text{A}/\text{cm}^2$ ) beyond  $\pm 11 \text{ cm}$ .

The end-to-end studies show manageable losses if we accept a scraper. Increasing the multipole lens aperture enables one to reduce the beam part dissipated on the scraper and may allow removing it. Specific studies would be needed on the scraper and the multipolar magnets. We managed some room for insertion of radioprotection walls against the losses at the end of the last long drift tube.

An uncorrected beam orbit in the last drift implies very strict and challenging dynamic tolerances on the previous elements. Some work is still needed to improve the design, for instance, optimizing the DTL aperture.

## REFERENCES

- [1] DSM/DAPNIA 03-72: CEA-DSM-DAPNIA-SACM, Contribution to the IFMIF KEP phase June 2000 to December 2002
- [2] IFMIF International Team, "IFMIF Comprehensive Design Report", January 2004
- [3] JAERI-Tech 2003-005, IFMIF-KEP, Key element technology phase report
- [4] J. Payet, BETA code, to be published.
- [5] F. Meot, T. Aniel, "Principles of the non-linear tuning of beam expander", NIM A379 (1996)
- [6] R. Duperrier, « Dynamique de faisceaux intenses dans les RFQs », Université Paris sud Orsay, n° 6194, juillet 2000
- [7] R. Duperrier, N. Pichoff, D. Uriot, "CEA Saclay codes review", ICCS conference, Amsterdam, 2002
- [8] N. Pichoff, J. M. Lagniel, and S. Nath, "Simulation Results with an Alternate 3D Space Charge Routine, PICNIC", Proceedings of the XIX International Linac Conference, p 141, Chicago
- [9] R. Duperrier, J. Payet, D. Uriot, "The IFMIF High Energy Beam Transport Line- Error studies", CEA Saclay DAPNIA-04-66 Rapport Interne.